

Room-temperature negative photoconductivity in degenerate InN thin films with a supergap excitation

Pai-Chun Wei,¹ Surojit Chattopadhyay,^{2,*†} Min-De Yang,³ Shih-Chang Tong,³ Ji-Lin Shen,³ Chien-Yao Lu,⁴ Han-Chang Shih,^{1,5} Li-Chyong Chen,⁶ and Kuei-Hsien Chen^{4,*‡}

¹*Department of Materials Science and Engineering, National Tsing Hua University, Hsinchu 30013, Taiwan*

²*Institute of Biophotonics Engineering, National Yang Ming University, Taipei 11221, Taiwan*

³*Physics Department, Chung Yuan Christian University, Chung-Li 320, Taiwan*

⁴*Institute of Atomic and Molecular Sciences, Academia Sinica, Taipei 10617, Taiwan*

⁵*Institute of Materials Science and Nano Technology, Chinese Culture University, Taipei 11114, Taiwan*

⁶*Center for Condensed Matter Sciences, National Taiwan University, Taipei 10617, Taiwan*

(Received 4 June 2009; revised manuscript received 8 November 2009; published 11 January 2010)

Negative photoconductivity (NPC), up to room temperature, has been observed in small band gap and degenerate (*n*-type) indium nitride (InN) thin films with superband-gap excitation of 2.3 eV. Samples investigated above 160 K showed bipolar behavior of photoconductivity with a fast positive response due to photo-generated electron and hole conduction in the valence and conduction band, respectively, followed by a slow relaxation below the dark-current background. However, below 160 K, the transient photoresponse was absolute negative with similar relaxation times. Hall measurements, under illumination, showed an increase in carrier density (*n*), but severe scattering in the charged recombination centers lowered the mobility (μ) and consequently a net $n\mu$ product controlling the PC. The NPC phenomenon in the degenerate system, not limited to InN, has been modeled on the basis of electronic scattering in the conduction band as against gap state transitions that controlled it in conventional nondegenerate semiconductors with subgap excitation.

DOI: [10.1103/PhysRevB.81.045306](https://doi.org/10.1103/PhysRevB.81.045306)

PACS number(s): 73.50.Pz, 71.55.Eq, 72.20.-i, 73.61.Ey

Indium nitride (InN) is an important member of the group III-V semiconductor family that is well known not only for their light-emitting properties but also for the emission tunability, over a broad spectral range, through band-gap engineering. The growing acceptance of the low band gap (0.6–0.7 eV) of InN is accompanied by the fact that it has the lowest effective mass of electrons and a resultant high mobility ($\mu \sim 4400$ and $30\,000$ cm²/V s at 300 and 77 K, respectively, for 2H InN) among all III-nitride semiconductors. The optical and transport properties gain significance more because InN is naturally *n*-type and degenerate. These interesting transport properties in InN can now be augmented with the observation of negative photoconductivity (PC) in it. Negative PC (NPC) is known to occur in low-band-gap semiconductors with activator impurities, such as gold-doped germanium,¹ as a result of sub-band-gap illumination. Although the first direct evidence of NPC came around 1954,¹ the scientists were in pursuit from 1951.^{2,3} Since then, it has been a rich history in NPC in semiconductors, such as Au-Ge alloys,¹ Co-doped silicon,⁴ *n*-InP,⁵ InAs,⁶ *p*-InSb,⁷ CdSe,⁸ *n*-PbTe,⁹ and γ -In₂Se₃,¹⁰ dealing with trap levels in the band gaps. Impurity-related photoabsorptions allowing electronic transitions between localized or extended states have been employed to explain the phenomenon. However, the subject is still in focus with recent studies in group III-V semiconductors¹¹ and quantum well heterostructures.^{12–14} Although the NPC effect in thin films is explained predominantly using electronic transitions,¹⁵ that in heterostructures, such as Ge/Si type II quantum dots,¹⁴ are based on tunneling of holes into the well or dot and trapping of electrons at the interface of the heterostructure thereby reducing the density of free electrons available for conduction.

Here we report on the observation of NPC in epitaxial

degenerate InN within the temperature range of $77\text{ K} < T \leq 300\text{ K}$ with unconventional superband-gap excitation. The origin of the NPC mechanism in degenerate InN is compared to conventional nondegenerate systems using sub-gap excitation, utilizing data from standard four-probe and photo-Hall measurement techniques. The distinction in the temperature-dependent PC transients in InN has been modeled qualitatively using electronic band transitions.

InN thin films, under investigation, were deposited at 550 °C via plasma-assisted molecular-beam epitaxy (PAMBE),¹⁶ using commercial *c*-sapphire/*c*-GaN (2 μ m) as substrates. Van der Pauw or the four-probe method was used for the Hall carrier concentration (*n*), mobility (μ), and photocurrent measurements on the samples. Coplanar Ohmic contacts of evaporated metallic In were made, using a shadow mask, on the InN film and subsequently soldered to a gold wire for PC measurements [inset, Fig. 1(a)]. The samples were loaded into a cryostat cooled to liquid-nitrogen temperatures and evacuated to 10⁻⁶ Torr. A continuous-wave (CW) excitation of 100 mW (8.5 W/cm²) Nd:yttrium aluminum garnet (YAG) laser (532 nm/2.33 eV) was used. A semiconductor characterization system¹⁷ (Keithley 4200-SCS) was utilized to measure the currents under 0.1 V external bias. Hall measurements were done in a conventional home-built system utilizing a 0.7 T electromagnet generating uniform magnetic field over 8 cm diameter. The temperature-controlled sample chamber was equipped with a quartz window for external oblique illumination. Band edges of the InN samples were estimated from optical-absorption measurements using Jasco V-57 UV/Vis/NIR spectrophotometer.

1.1- μ m-thick InN thin films,¹⁶ having 0.7 eV absorption band edge at 300 K and carrier density (*n*) of $\sim 3.85 \times 10^{18}$ cm⁻³, are the subject of this investigation. Figure 1(a)

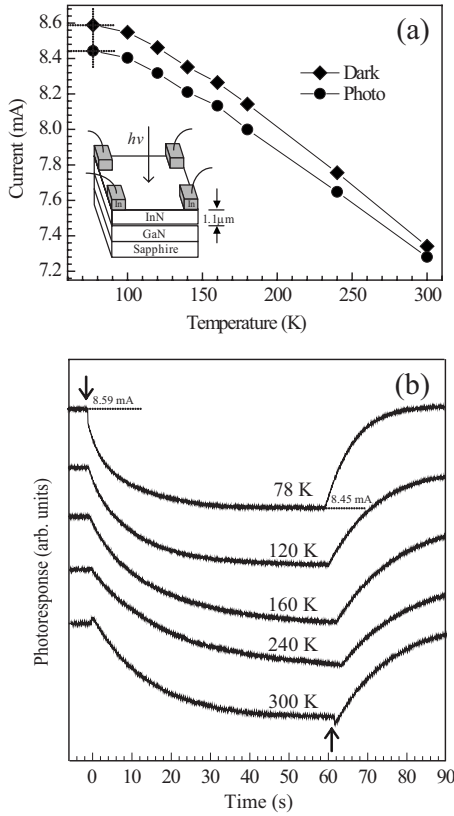


FIG. 1. (a) Steady-state dark and saturated photocurrents measured in InN sample as a function of temperature. A schematic of the sample geometry is shown in the inset. (b) Single cycle photocurrent transient response of InN measured at different temperatures with illuminations on and off marked by \downarrow and \uparrow , respectively, on the time axis. Steady-state dark-current and saturated photocurrent values are shown by the dashed lines for the measurement at 78 K. The absolute dark (\blacklozenge) and photocurrent (\bullet) values could be estimated from (a) (shown also by the dashed lines). Similarly, the absolute current values could be estimated from (a) for all measurement temperatures. All photocurrent transients are shifted vertically for clarity. The vertical axis in (b) does not represent absolute current values. Note that the saturated photocurrent is user defined.

shows the variation of dark and photocurrent¹⁷ in InN, as a function of temperature (T), measured by the four-probe method with a sample geometry shown in the inset. InN demonstrates a metallic behavior in the dark due to its inherent degeneracy. Interestingly, it shows a distinct drop in photocurrent with respect to the steady-state dark current at all temperatures within $77 \text{ K} < T \leq 300 \text{ K}$. This is the evidence of NPC with superband-gap excitation in InN. The temperature dependence of the PC transients is shown in Fig. 1(b) that demonstrates similar overall negative photoresponse but with two characteristic differences above and below 160 K. This behavior is cyclic and repeatable over several on-off cycles.¹⁸

Macroscopically, a faster decay of the PC and faster recovery of the persistent NPC to the steady-state dark-current value was observed at lower temperatures than at higher temperatures. However, both relaxations have a time scale of seconds. Such long relaxation times are quite common in materials that demonstrate a defect-induced NPC.^{9,15,19} Mi-

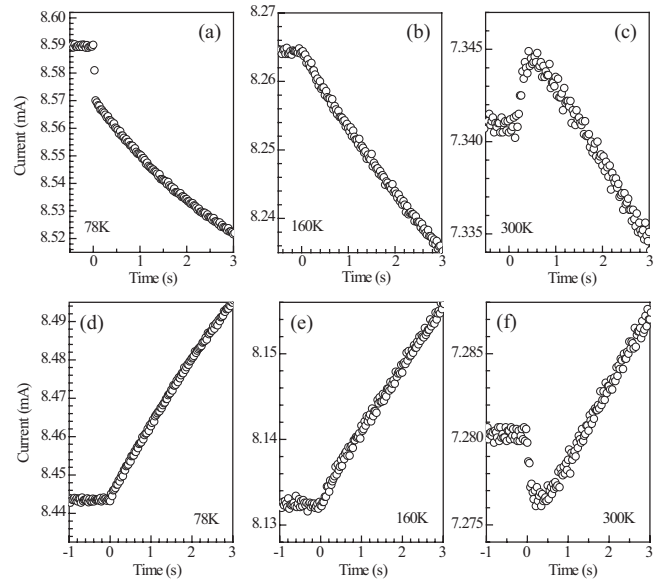


FIG. 2. Higher time resolved photocurrent transient response in InN thin film sample after illuminations [(a)–(c)] on and [(d)–(f)] off, measured at different temperatures.

croscopically, the finer details of the PC transients, instantaneously after the on [Figs. 2(a)–2(c)] and off [Figs. 2(d)–2(f)] states of illumination, show distinctive behavior at low and high temperatures. At lower temperatures ($< 160 \text{ K}$), one observes an absolute NPC with two relaxation times, fast at the onset of illumination and then a rather slow decay to saturation [Fig. 2(a)]. For $T < 160 \text{ K}$, the persistent NPC recovered to attain the steady-state dark-current values in approximately $\sim 24 \text{ s}$ after the illumination is shut off [Fig. 2(d)]. In contrast, at higher temperatures ($> 160 \text{ K}$) with illumination on, we observed an instantaneous positive current [Fig. 2(c)], which saturates in $\sim 300 \text{ ms}$ and its magnitude increasing with T , followed by a slow decay to the NPC regime [Fig. 2(c)]. This is followed by a similar recovery to the steady-state dark-current value [Fig. 2(f)] in $\sim 32 \text{ s}$ after the illumination is shut off. The small bumps in the PC transients instantaneously after illumination is on [Fig. 2(c)] or off [Fig. 2(f)], for $T > 160 \text{ K}$, are due to photogenerated electron and hole conduction in the conduction and valence band, respectively, of InN as we will see later. At $T = 160 \text{ K}$, only the slow decay to the NPC regime was observed with no positive photocurrent [Fig. 2(b)].¹⁸ Consequently, no bump in the transient response showed up when the illumination was shut off [Fig. 2(e)]. The long-time scales of PC decay and recovery to the steady state could have been an artifact of increased temperature upon laser irradiation. To estimate the local sample temperature, ambient (300 K) micro-Raman spectroscopy was performed with a similar Nd-YAG laser (focused to a $2 \mu\text{m}$ spot size) with tunable power density. The ratio of the Stokes and anti-Stokes lines [E_2 (high) at 491 cm^{-1}] yielded a temperature increases of 40 and 32 K when laser power densities of 2.5 and 2.2 MW/cm^2 were used, respectively. No anti-Stokes line could be observed with a laser power density of $3 \times 10^4 \text{ W}/\text{cm}^2$. Power-dependent PC transient measurements (Fig. 3) were carried out at room temperature for cor-

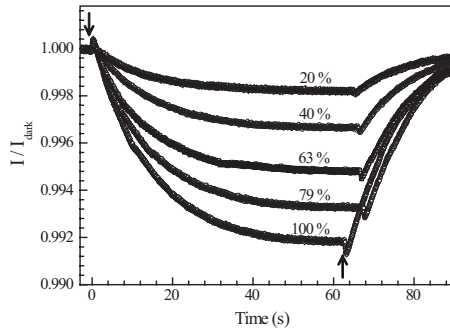


FIG. 3. Power-dependent PC transients of InN thin film carried out at 300 K. The vertical axis corresponds to the ratio of instantaneous current (photo or dark) to the steady-state dark current. Illuminations on and off are marked by \downarrow and \uparrow , respectively, on the time axis. Note that the saturated current ratio (I/I_{dark}) is user defined.

roborative evidence. At even 20% of the total power density (i.e., 1.7 W/cm^2), the NPC was clearly observed. Considering the bulk thermal-conductivity values for InN and the sample geometry used, a temperature change of $\sim 10 \text{ K}$ could be estimated over 50 s, assuming 100% radiation absorption (neglecting power attenuation and reflection losses). However, for the dark conductivity to approach the lower photoconductivity values, temperature increases of $>30 \text{ K}$ and $\sim 20 \text{ K}$ were required for the low ($<160 \text{ K}$) and high ($>160 \text{ K}$) measurement temperatures, respectively [Fig. 1(a)]. At lower incident powers, the temperature change will be much lower than 10 K, but NPC was still observed (Fig. 3). In addition, the NPC signal is observed within milliseconds of laser irradiation [Fig. 2(a)]. Hence, the NPC signal is not a predominantly thermal artifact since any temperature change in the InN sample with 8.5 W/cm^2 radiation can be considered insignificant. However, small it may be, the thermal contribution, especially to the long tail of the transient, cannot be separated, from the optical effects, or ruled out in our study.

The nature of this PC variation is similar to several materials that demonstrated NPC, such as Co-doped silicon,¹⁵ $\gamma\text{-In}_2\text{Se}_3$,¹⁰ and heterojunction-type devices.¹³ However, those materials were nondegenerate and showed NPC under subband-gap illumination. In contrast, this study involved degenerate InN with superband-gap illumination which should logically increase n in the conduction band (E_C) producing a positive PC, however small (in magnitude) it may be. Hall measurements (Fig. 4) did show an increase in n under illuminated conditions than in the dark at all measurement temperatures [Fig. 4(b)]. Interestingly, however, μ showed a decrease under illuminated conditions [Fig. 4(c)] at all temperatures and so does the product $n\mu$ [Fig. 4(d)] that controls the overall PC. This is indeed possible in degenerate InN due to large electron scattering in charged recombination centers. This is where the NPC in InN significantly differs from the conventional nondegenerate systems reported earlier. In addition, the temperature-dependent features of the transient PC response also required a modeling involving electron band transitions that was used to explain the NPC in the nondegenerate systems.

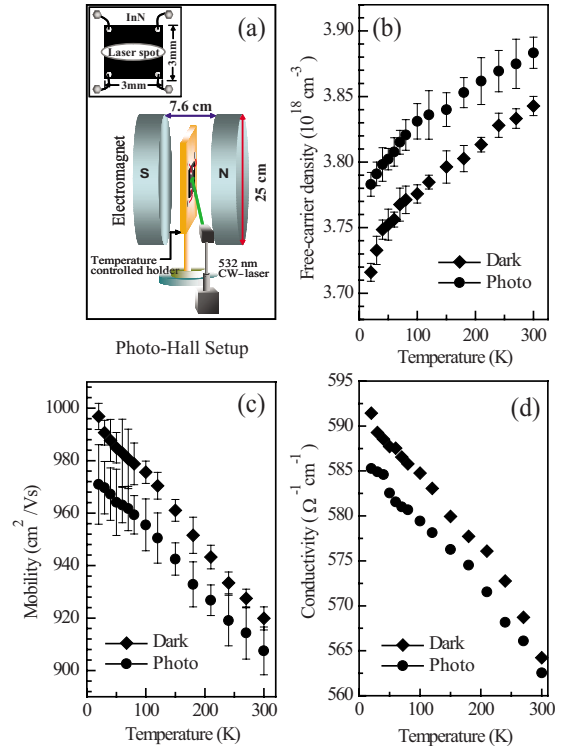


FIG. 4. (Color online) (a) A schematic of the Hall measurement setup using a 532 nm laser as excitation (photo-Hall measurement). (b) Free carrier density (n), (c) mobility (μ), and (d) the product $\sigma=en\mu$, e being electronic charge, measured as a function of temperature under dark and illuminated conditions using the photo-Hall setup. Error bars in (b) and (c) represent scatter of data over ten separate measurements.

In order to explain the features in the transient photoreponse, one has to assume an energy-band model (Fig. 5) for low band gap and degenerate (high carrier concentration) InN with the Fermi level (E_{Fn}) inside the E_C . InN is unintentionally doped and contains random impurities, such as oxygen, in addition to inherent electronic or structural defects expressed as states within the band gap and band tails.²⁰⁻²³ We assumed recombination centers (E_R) in the band gap (0.7 eV) of InN. Presence of states above the E_C minimum²⁴ may also play some role in containing the n

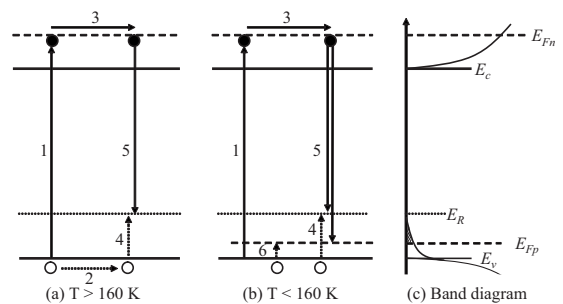


FIG. 5. Energy-level diagrams showing electronic transitions responsible for the photocurrent transient response shown in Figs. 1 and 2. (a) At $T > 160 \text{ K}$ and (b) at $T < 160 \text{ K}$ for degenerate InN sample with superband-gap excitation. (c) A general energy-band diagram for InN illustrating different band positions.

value. In this scheme, E_{Fn} and E_{Fp} represent the electron and hole quasi-Fermi-level, respectively. Light can excite the electrons from the valence band (E_V) [process 1, Fig. 5(a)], leaving holes behind which diffuses along with electrons in the conduction band [processes 2 and 3, Fig. 5(a)] therein to produce the positive PC. The diffusing holes will recombine at E_R [process 4, Fig. 5(a)], making them positively charged scattering centers for the electrons. At high temperatures ($T > 160$ K), the hole quasi-Fermi-level, E_{fp} , is pushed inside E_V enabling the holes to conduct easily before being captured at E_R . The rate of hole trapping at E_R being slower at high temperatures, an instantaneous positive PC, is observed due to the photogenerated electrons in the E_C . With time, scattering at charged E_R reduces electron mobility resulting in NPC. However, at low temperatures ($T < 160$ K), the E_{Fp} is in the gap, (for example, at 10 K, E_{Fp} is 7 meV above E_V , Figs. 5(b) and 5(c)) (Refs. 20 and 25) and the nonequilibrium holes localize quickly at E_R and E_{Fp} [processes 4 and 6, Fig. 5(b)] and an instantaneous NPC is observed. When processes 4 and 6 dominates over processes 2 and 3 [Fig. 5(b)], the positive PC is suppressed, especially for $T < 160$ K. Hence, the temperature-dependent hole trapping at E_R and tail states near E_{Fp} are key to this phenomenon. The negative difference in the $n\mu$ value, under illuminated and dark conditions, exceeds the photogenerated carrier contributed positive PC at any given temperature, within the range studied, and results in NPC. In contrast, to explain NPC in conventional nondegenerate semiconductors, at least two gap states, donor and acceptor type, filled or partially filled, had to be introduced.⁴ In nondegenerate semiconductors, electrons de-exciting from E_C [process 4, Figs. 5(a) and 5(b)] limits the buildup of n in E_C , thereby slowly saturating the $n\mu$ and the resultant NPC.

With illumination turned off, the photogenerated current contributing to the positive PC decays causing a further drop in the net conductivity. This feature is clearly seen only for $T > 160$ K (say 240 or 300 K) where the photocarrier-assisted positive PC was observed [Fig. 2(f)]. Hereafter, the remaining nonequilibrium electrons in E_C decays persistently [process 5, Figs. 5(a) and 5(b)], with a longer time scale, recovering the current to the initial (dark) steady-state level. At low temperatures, this recovery process may be faster [Fig. 1(b)]. A qualitative modeling of the observed data is hence achieved through the abovementioned mechanism.

In conclusion, we observed negative photoconductivity up to room temperature in degenerate n -type InN thin films with superband-gap excitation. Hall measurements, under illumination, showed that a scattering-induced decrease in carrier density and mobility product contributed to the negative photoconductivity compared to the dark. The transient photocurrent response indicates that the contribution of positive and negative photoconductivities comes through photogenerated carriers in the continuous bands above 160 K and electron scattering in the charged recombination centers, respectively. This is in contrast to the gap state transitions responsible for negative photoconductivity in conventional nondegenerate semiconductors that employed subgap excitation. The proposed model could explain the observed negative photoconductivity results satisfactorily in degenerate InN system in particular and most likely other degenerate systems in general.

We acknowledge financial support from National Science Council, Ministry of Education in Taiwan as well as the U.S. AFOSR-AOARD. The authors are grateful to L. W. Du (National Sun Yat-Sen University, Taiwan) for providing the InN thin-film sample.

*Corresponding author.

†sur@ym.edu.tw

‡chenkh@pub.iams.sinica.edu.tw

¹R. Newman, Phys. Rev. **94**, 278 (1954).

²J. R. Haynes and W. Shockley, Phys. Rev. **81**, 835 (1951).

³W. C. Dunlap, Jr., Phys. Rev. **91**, 1282 (1953).

⁴C. M. Penchina, J. S. Moore, and N. Holonyak, Phys. Rev. **143**, 634 (1966).

⁵A. Berkeliyev and K. Durdyev, Sov. Phys. Semicond. **5**, 646 (1971).

⁶L. A. Balagurov, É. M. Omel'yanovskii, and V. I. Fistul, Sov. Phys. Semicond. **12**, 557 (1978).

⁷I. M. Ismailov, D. N. Nasledov, M. A. Sipovskaya, and Yu. S. Smetannikova, Sov. Phys. Semicond. **3**, 1154 (1970).

⁸R. H. Bube, Phys. Rev. **99**, 1105 (1955).

⁹B. A. Akimov, V. A. Bogoyavlenskiy, L. I. Ryabova, and V. N. Vasilkov, Phys. Rev. B **61**, 16045 (2000).

¹⁰R. Sreekumar, R. Jayakrishnan, C. S. Kartha, and K. P. Vijayakumar, J. Appl. Phys. **100**, 033707 (2006).

¹¹O. E. Raichev and F. T. Vasko, Phys. Rev. B **73**, 075204 (2006).

¹²A. S. Chaves and H. Chacham, Appl. Phys. Lett. **66**, 727 (1995).

¹³A. L. Powell, C. C. Button, J. S. Roberts, P. I. Rockett, H. G. Grimmeiss, and H. Pettersson, Phys. Rev. Lett. **67**, 3010 (1991).

¹⁴A. I. Yakimov, A. V. Dvurechenskii, A. I. Nikiforov, O. P. Pchelyakov, and A. V. Nenashev, Phys. Rev. B **62**, R16283 (2000).

¹⁵M. C. P. Chang, C. M. Penchina, and J. S. Moore, Phys. Rev. B **4**, 1229 (1971).

¹⁶C. L. Hsiao, L. W. Tu, M. Chen, Z. W. Jiang, N. W. Fan, Y. J. Tu, and K. R. Wang, Jpn. J. Appl. Phys. **44**, L1076 (2005).

¹⁷R. S. Chen, H. Y. Chen, C. Y. Lu, K. H. Chen, C. P. Chen, L. C. Chen, and Y. J. Yang, Appl. Phys. Lett. **91**, 223106 (2007).

¹⁸See supplementary material at <http://link.aps.org/supplemental/10.1103/PhysRevB.81.045306> for the cyclic and repetitive behavior of the photocurrent transient over several on-off cycles, and for a schematic of the transient photocurrent response with indicative time scales.

¹⁹E. Skipetrov, E. Zvereva, L. Skipetrova, and E. Slyn'ko, Physica B **302-303**, 393 (2001).

²⁰B. Arnaudov, T. Paskova, P. P. Paskov, B. Magnusson, E. Valcheva, B. Monemar, H. Lu, W. J. Schaff, H. Amano, and I. Akasaki, Phys. Rev. B **69**, 115216 (2004).

²¹P. V. Miegheem, Rev. Mod. Phys. **64**, 755 (1992).

²²M. Petracic, P. N. K. Deenapanray, M. D. Fraser, A. V. Soldatov, Y.-W. Yang, P. A. Anderson, and S. M. Durbin, J. Phys. Chem. B **110**, 2984 (2006).

²³X. Xu, P. Specht, R. Armitage, J. C. Ho, E. R. Weber, and C.

- Kisielowski, Appl. Phys. Lett. **87**, 092102 (2005).
- ²⁴L. H. Dmowski, J. A. Plesiewicz, T. Suski, H. Lu, W. Schaff, M. Kurouchi, Y. Nanishi, L. Konczewicz, V. Cimalla, and O. Ambacher, Appl. Phys. Lett. **86**, 262105 (2005).
- ²⁵G. W. Shu, P. F. Wu, M. H. Lo, J. L. Shen, T. Y. Lin, H. J. Chang, Y. F. Chen, C. F. Shih, C. A. Chang, and N. C. Chen, Appl. Phys. Lett. **89**, 131913 (2006).